ELSEVIER

Journal of Chromatography A, 740 (1996) 1–9

JOURNAL OF CHROMATOGRAPHY A

Comparison of an ordered mesoporous aluminosilicate, silica, alumina, titania and zirconia in normal-phase high-performance liquid chromatography[1]

M. Grün[a], A.A. Kurganov[a], S. Schacht[b], F. Schüth[b], K.K. Unger[a,*]

[a]*Institut für Anorganische und Analytische Chemie, Johannes Gutenberg-Universität, Becherweg 24, D-55099 Mainz, Germany*

[b]*Institut für Anorganische Chemie, Johann Wolfgang Goethe-Universität, Marie Curie Str. 11, D-60439 Frankfurt/M., Germany*

Received 30 November 1995; revised 26 February 1996; accepted 4 March 1996

Abstract

This paper investigates the behaviour of silica, alumina, titania, zirconia and the novel mesoporous aluminosilicate MCM-41 in normal-phase high-performance liquid chromatography under comparable conditions. The physicochemical properties of the oxides and MCM-41 are described. MCM-41 is an ordered mesoporous material with a regular pore structure composed of an assembly of hexagonal tubes with a pore diameter of 4 nm. In chromatography MCM-41 exhibits acid and basic properties and proves to be suitable for the separation of acid, neutral and basic compounds.

Keywords: Stationary phases, LC; Silica; Zirconia; Aluminosilicate; Alumina; Titania; MCM-41

1. Introduction

Although silica is the dominating packing material in high-performance liquid chromatography (HPLC) the potential of other oxides has not yet been fully exploited. Attempts have been made to manufacture spherical porous alumina and to use it in its native form or with lipophilic polymeric coatings in reversed-phase (RP) HPLC [1,2]. The accumulated knowledge on oxides in the ceramic industry has led to the development of microparticulate porous crystalline zirconias with defined properties and high chemical and mechanical stability [3]. Zirconia modified with polymer and carbon coatings has been thoroughly investigated in RP-HPLC. Recently, interest has focused on porous crystalline titania (anatas) as packing to be used in normal-phase, RP and ion-exchange HPLC [4].

It appears that high-quality packings can be manufactured with respect to column efficiency, column stability and column regeneration. However, each oxide possesses its own surface chemistry which requires extended knowledge and experience to be successfully applied in HPLC.

In 1992 the researchers of the Mobil Oil Corporation reported on a new family of ordered mesoporous materials, called M41 S [5,6]. The most popular

* Corresponding author.

[1] Paper presented at the *19th Int. Symp. on Column Liquid Chromatography and Related Techniques, 28 May–2 June, 1995, Innsbruck, Austria.*

0021-9673/96/$15.00
PII S0021-9673(96)00205-1

member of this family is the MCM-41 (matter of composition of material 41) exhibiting a unidimensional hexagonal array of hexagonally shaped mesopores. The bulk is composed of amorphous silica and aluminosilicate. The pore diameter can be varied between 2 and 8 nm. MCM-41 shows some interesting features as compared to mesoporous crystalline and amorphous oxides: (i) the unique pore structure; (ii) the mild Broensted acidity; (iii) the isomorphous substitution of silicon by other elements, eg., aluminium, titanium etc.

A large amount of literature has been published on the formation mechanism of MCM-41 and on its physicochemical characterisation [7,8]. Recent examinations on the pore structure of MCM-41 revealed that the material contains highly ordered regimes with hexagonally shaped pores but also less ordered regimes with a lamellar or disordered structure [9]. The aim of this paper is to report for the first time on the properties of MCM-41 packings in normal-phase HPLC and to compare its retention behaviour and selectivity with other oxide packings.

2. Experimental

2.1. Materials

MCM-41 was prepared according to the procedure given by Beck [6] as purely siliceous compound and as aluminosilicate with adjusted Si/Al ratios.

2.1.1. Procedure 1: siliceous MCM-41

A 500-cm^3 volume of a *n*-cetyltrimethylammonium chloride in water (25%, w/w, Aldrich, Steinheim, Germany) was added to 38.5 g of tetramethylammonium bromide (98%, w/w, Aldrich) and stirred for 30 min until a homogeneous solution was obtained. A mixture of 90.87 g of a sodium silicate solution in water (27%, w/w, of SiO_2, 8.3%, w/w, of NaOH, Woellner, Ludwigshafen, Germany), 62.5 g of Aerosil 200 (Degussa, Hanau, Germany) and 500 cm^2 of deionized water were added and agitated overnight. The suspension was heated at 160°C for three days. After cooling to room temperature the product was filtered and washed with copious amounts of deionized water and allowed to air dry. The dry mass was carefully ground using a mortar and a pestle and placed in a wide-bottomed ceramic bowl. The sample was calcined in air at 500°C at a heating rate of 2°C/min for a period of 12 h.

2.1.2. Procedure 2: aluminosilicate MCM-41 (Si/Al ratio: 60)

The procedure is essentially the same as for sample 1. A 1.45-g amount of pseudo-boehmite AlO(OH), Pural SB (Condea, Hamburg, Germany) was added to the template solution as the alumina source.

MCM-41 samples with different Si/Al ratios were synthesized accordingly, using appropriate amounts of pseudo-boehmite.

The materials were characterised by X-ray diffraction (XRD) (Seiffert 3000 APD diffractometer) with a Cu $K_{\alpha 1}$ radiation of 0.154 nm between $0° < 2\Theta < 25°$, transmission electron microscopy (TEM) (JEOL 4000 EX microscope operated at 400 kV) and NS at 77 K (ASAP 2000, Micromeritics, Neuss, Germany).

The pK_a values of MCM-41 were determined in 0.1 *M* NaCl solutions. The pH stability was estimated by XRD measurements after treatment with buffer solutions of various pH. pH_{pzc} values were obtained by ζ-potential measurements.

The other oxides were supplied by E. Merck, Germany (LiChrospher Si 100, Aluspher-100, zirconia) and YMC Europe, Germany (titania).

2.2. HPLC measurements

MCM-41 was treated before use by grinding in a mortar followed by repeated sedimentation in 2-propanol. A fraction with a particle diameter of approx. 5–10 μm was obtained as controlled by scanning electron micrographs.

All columns of 250×4 mm were packed by means of the slurry technique using a 2% (w/w) slurry of the appropriate oxide in 2-propanol or acetone. The maximum pressure during the filling process was about 500 bar.

After packing the columns were equilibrated using a mixture of *n*-hexane–isopropanol (95:5, v/v) saturated with water.

A mixture of *n*-hexane–2-propanol (99.5:0.5, v/v) was used as standard eluent. Polycyclic compounds were separated using *n*-pentane as eluent.

The HPLC equipment consisted of a chromato-

graphic pump (Model LC-655A-12, Merck-Hitachi, Germany), a variable-wavelength UV detector operated at 250 nm (Shimadzu, Japan) and a Rheodyne injection valve (Model 7125, Rheodyne, USA).

The test mixtures were prepared from compounds of analytical grade obtained from Merck (Germany) or Aldrich (Germany).

3. Results and discussion

3.1. Physicochemical characterisation of MCM-41 and comparison with oxides

Table 1 presents some common properties of oxides and MCM-41. The determining factor controlling the chemistry of oxides as well as that of MCM-41 is the coordination of metal atom(s) linked to oxygen and is related to the bulk structure of the material.

In amorphous silica, silicon is tetrahedrally coordinated. The X-ray pattern generally shows broad reflections around $2\Theta \approx 11°$ which may become sharper after a post-treatment of the parent produced by means of hydrothermal, acid or heat treatment [10].

Depending on the starting material and the type of manufacturing process, porous alumina can be amorphous (AluSpher, E. Merck) or crystalline (γ-alumina, Unispher, Biotech). In both products aluminium is mainly octahedrally coordinated which has been proved by ^{27}Al magic angle spinning (MAS) nuclear magnetic resonance (NMR) spectroscopy [11].

Titania used as chromatographic packing (YMC Europe) exhibits the crystalline structure of anatas with a coordination number of titanium of 6. The X-ray pattern of the various titania brands (YMC Ti-100, Ti-300, Ti-1000) also allows one to estimate the crystallite size based on the sharpness of the reflections [10].

Zirconia exists in three crystalline modifications; tetragonal, cubic and monoclinic [3]. The zirconia packing manufactured by the 3M Corporation is monoclinic in which zirconium atoms are heptacoordinated to oxygen. Closer inspection indicates tri- and tetracoordinated oxygen.

The high coordination numbers of Ti–O and Zr–O are responsible for the strong complexation properties of these oxides which is reflected by ligand exchange and ion-exchange reactions.

The surface chemistry of metal oxides is characterised by their acidity and basicity which are of Broensted and Lewis base types and by their ion-exchange properties. The latter are determined by the pH where the particles bear a zero charge. It should be emphasized that the pH given in Table 1 has a precision of about ± 2 units and is strongly dependant on how the oxide is manufactured and on the method by which the pH_{pzc} was determined. As a

Table 1
Properties of oxides and MCM-41

	Silica	Alumina	Titania	Zirconia	MCM-41
Coordination number of Me–O	4	6	6	7	4(6)
Bulk structure	Amorphous	Crystalline and amorphous	Crystalline	Crystalline	Amorphous
Acid–base properties	Weak Broensted acidity	Low Broensted acidity, weak Lewis acidity and basicity	Strong Lewis acidity and basicity, strong Bronsted acidity	Pronounced lewis acidity and basicity	Low Broensted acidity, low Lewis acidity
pK_a of Broensted sites	7	8.5	0.5–2.0 (anatas)	10–13	7.2 (Si/Al>1000) 8.2 (Si/Al=9)
pH of zero charge pH_{pzc}	3	7	5	8	
pH-stability range	2–8	2–12	1–14	1–14	2–9

general rule, above the pH_{pzc} the metal oxide behaves as a cation-exchanger, below the pH_{pzc} the metal oxide exerts anion-exchange properties.

Amorphous porous silica has a weak Broensted acidity due to the silanol groups [12]. At higher temperatures, silica can develop a Lewis acidity and basicity due to siloxane groups activated during the course of dehydration according to the reactions:

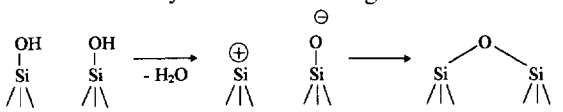

Porous alumina subjected to a calcination above 500°C provides a Lewis acidity and a basicity as well as a low concentration of Broensted acid sites. Broensted and Lewis acid sites are identified by adsorption of pyridine using infrared (IR) spectroscopy [13]

Titania exhibits a pronounced Lewis acidity and basicity, anatas possesses the highest Broensted acidity of all oxides. The acid–base properties of zirconia have been treated in depth by Nawrocki et al. [3]. Zirconia exerts a strong Lewis acidity and basicity due to unsatisfied zirconium and oxygen atoms at the surface. Zirconia also contains weakly acid hydroxyl groups. The pK_a of Broensted acid sites of metal oxides can be determined spectroscopically on the basis of the wave length shift, $\Delta\nu$OH, upon the adsorption of benzene [14,15]. It is seen that zirconia has the weakest Broensted acidity of all oxides followed by γ-alumina and silica. Yates [16] has proposed a simplified model of the surface of oxides with the surface equilibria and the intrinsic ionisation constants involved:

$$M-OH_2^+ \underset{+H^-}{\overset{K_{a_1}^{int}}{\rightleftarrows}} M-OH \underset{+H^+}{\overset{K_{a_2}^{int}}{\rightleftarrows}} M-O^-$$

The pH_{pzc} is related to the ionization constants $K_{a_1}^{int}$ and $K_{a_2}^{int}$ by the following equation:

$$pH_{pzc} = 0.5(pK_{a_1}^{int} + K_{a_2}^{int}) \quad (1)$$

with

$$pK_{a_1}^{int}(pK_{a_2}^{int}) = -\log_{10} K_{a_1}^{int}(K_{a_2}^{int}) \quad (2)$$

Eq. (1) means that at $pH < pK_{a_1}^{int}$ the oxide acts as an anion exchanger and at $pH > pK_{a_2}^{int}$ it acts as a cation exchanger.

In more detail, the ion-exchange properties of oxides are much affected by the adsorption of ions and ligand exchange properties involving water as ligand as exemplified by Nawrocki et al. [3] for zirconia.

In the context of the bulk and surface structure, there are large differences between metal oxides in chemical stability towards acidic and alkaline solutions. Amorphous silica covers the smallest pH range with respect to chemical stability (pH 2–8), followed by γ-alumina (pH 2–12). Both titania (anatas) and crystalline monoclinic zirconia exhibit an excellent pH stability (pH 1–14) which is an important aspect for the regeneration of these oxides in the usage of HPLC packings.

Gradations are also observed in the bulk density of metal oxides which increases in the following sequence: Silica (2.2 cm^3/g), alumina (3.5 cm^3/g), titania (4 cm^3/g) and monoclinic zirconia (5.8 cm^3/g). The higher the bulk density the higher will be the mechanical stability of particles and the more stable will be the chromatographic column bed. The latter feature is less significant for the use of columns in analytical HPLC but more relevant for columns in preparative and process HPLC.

With the current manufacturing processes, the named metal oxides can be synthesized as microparticulate packings of a mean particle diameter, d_p, between 5–10 μm with a controlled mean pore diameter between 10–100 nm and specific surface area, a_s (BET), between 5–200 m^2/g. Specific data on these materials are presented in Table 2.

Compared to silica, the specific pore volume, V_p, of alumina and more so for titania and zirconia is low (between 0.1–0.5 cm^3/g). However, in a comparison of metal oxides as packings in HPLC, one must relate the a_s (BET) and V_p values to the unit of column volume, i.e., the a_s (BET) and V_p values must be multiplied by the packing density in g per unit column volume of the given material. Doing that, the a_s (BET) and V_p values per unit column value become similar to those of porous silica due to the much higher packing densities of alumina, titania and zirconia (>1 g/cm^3) than of silica (0.5 g/cm^3).

Although MCM-41 is a novel material, much research has been carried out to elucidate its bulk structure, surface chemistry and pore structure [17].

As indicated by XRD and TEM measurements,

Table 2
Properties of packing materials

	Silica	Alumina	Titania	Zirconia	MCM-41
Particle diameter, μm	5	5	5	10	5–10
Specific surface, m^2/g	352	155	51	52	615
Specific pore volume, cm^3/g	1.23	0.5	0.16	0.24	0.68
Diameter of pores, nm	14	13	12.3	18.1	4.4

MCM-41 provides an ordered structure composed of hexagonally packed pores with a hexagonal pore shape. However a closer inspection of probes of the same sample also indicate regions with a less ordered structure [9].

In the XRD pattern, four Bragg peaks can be distinguished below $2\Theta \approx 7°$ which can be indexed in P6 symmetry as (100), (110), (200), (210) and (300). There are no peaks with $1 \neq 0$ indicating that there is no long range order in the direction of the channel axis. The first reflex at (100) is used to calculate the pore diameter assuming a wall thickness of about 1 nm. The pore walls are amorphous. The purely siliceous MCM-41 contains tetrahedrally linked silicon atoms units with silanol groups as Broensted acid sites. In the case of the aluminium containing MCM-41, the ^{27}Al MAS-NMR spectrum shows two peaks around 0 and 50 ppm which are assigned to tetrahedrally and octahedrally coordinated aluminium [18]. The octahedrally coordinated aluminium may originate from the removal of aluminium from the pore walls to alumina oxide hydrate species being located in the channels. Tetrahedrally coordinated aluminium causes a high Broensted acidity as compared to zeolites.

IR spectroscopy measurements with pyridine and ammonia have indicated that MCM-41 possesses a moderate Broensted acidity as observed in amorphous alumosilicate. In contrast to amorphous alumosilicate, the Lewis acidity is appreciably higher [18].

Apart from the regularly shaped pores whose diameter can be varied between 2 and 8 nm depending on the synthesis conditions, the other unique feature of MCM-41 is the texture of the particle. The material as made is composed of agglomerates of 10–100 μm in size. From electron microscopy (scanning and transmission), it can be seen that the agglomerations are made of primary particles of about 50–100 nm in size. In other words, the regular pore structure is present only in these primary particles.

Based on NS data and the *t*-plot, an "intracrystalline" specific surface area of 950 ± 20 m^2/g and an "intercrystalline" specific surface area of about 100 ± 20 m^2/g was calculated for a 4 nm pore size material [19]. The external a_s (BET) value of about 100 m^2/g is in accordance with particles of 50 to 100 nm in size.

The strength of agglomeration is not very high so that care is required at the grinding of the material to obtain 5–10 μm fractions. Also, a large number of fines are produced due to grinding which can be removed by sedimentation.

The bimodal pore size distribution and the agglomerate structure of particles favours the mass transfer kinetics when MCM-41 is used as packing material in HPLC. The interstitial pores of about 50 nm in size serve as transport pores to the internal pores of about 4 nm in size. This is seen reflected in the rather symmetrical peaks of analytes used in the HPLC experiments.

For MCM-41, a packing density of 0.25 g/cm^3 of column volume can be measured indicating the rather irregular shape of the particles. This is confirmed by scanning electron micrographs of the sedimentated material. The low packing density is partly compensated by the high specific surface area (950 m^2/g) of MCM-41 so that the BET area per column becomes comparable to those of the other oxides.

3.2. Behaviour of oxides and MCM-41 in normal-phase chromatography

3.2.1. Separation of basic compounds

Fig. 1 shows the separation of anilines and pyridines on alumina (A), zirconia (B) and titania

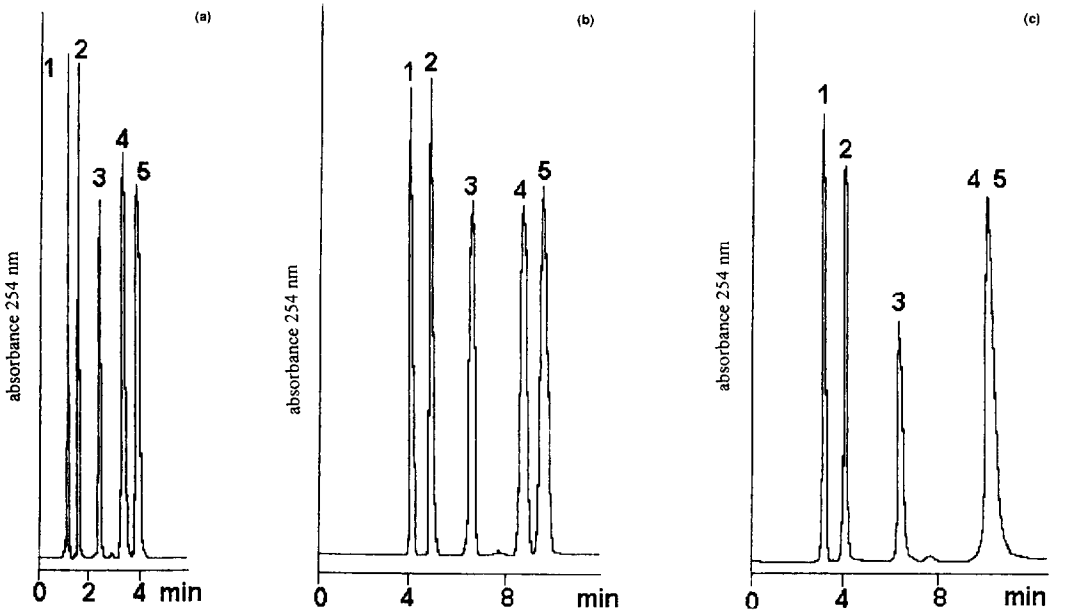

Fig. 1. Separation of a mixture of basic compounds on alumina (a), zirconia (b) and titania (c). Columns: 125×4 mm (a); 250×4 mm (b, c). Eluent: *n*-hexane–2-propanol (99.5:0.5, v/v). Flow-rate: 1 cm^3/min. UV detection at 254 nm. Injection volume: 20 mm^3. Peaks: 1 = N,N-dimethylaniline; 2 = N-methylaniline; 3 = 2-methylpyridine; 4 = 4-methylpyridine; 5 = aniline.

(C). The rather short retention times of analytes and the symmetrically shaped peaks clearly indicate the basic character of these oxides in chromatography.

Fig. 2 displays the separation of anilines on LiChrospher Si 100 (a), MCM-41 (Si/Al ratio = 9) (b) and MCM-41 (Si/Al ratio > 1.000) (c). Due to interactions with Broensted acidic sites present on these materials, the retention times are much longer than those measured using alumina, zirconia and titania. In the case of MCM-41, all peaks are nearly symmetrical especially when using the sample with a Si/Al ratio of 9 whereas LiChrospher Si 100 exhibits some tailing especially when eluting aniline.

The difference between MCM-41 and silica on one side and zirconia, titania and alumina on the other becomes even more obvious when looking at the separation of pyridines. These compounds could not be eluted on LiChrospher Si 100 and MCM-41 using *n*-hexane–2-propanol (99.5:0.5, v/v) as eluent (not shown). However, a separation could be achieved on both MCM-41 and LiChrospher Si 100 using a mixture of methylene chloride–methanol (95:5, v/v). Although in both cases tailed peaks were obtained, MCM-41 shows a better peak shape whereas the separation on silica is not satisfactory.

3.2.2. Separation of neutral compounds

As model substances for the behaviour against neutral compounds polycyclic aromatic hydrocarbons were chosen. Due to their π-electron system, polycyclic aromatic hydrocarbons behave as Lewis bases and so interactions with Lewis acidic sites located on the packing material become dominant for retention.

Silica shows almost no retention due to the lack of Lewis acid sites. When using MCM-41 as packing material, one can see that the hydrocarbons are much more retarded by the purely siliceous (not shown) as well by the aluminosilicate material (Fig. 3a) This behaviour may be due to the formation of Lewis acidic siloxane bridges during calcination and in the case of the aluminium containing sample, formation of Lewis acidic extra framework aluminium.

As can be seen from Fig. 3b–3d alumina, titania and zirconia show well resolved peaks due to the presence of Lewis acidic sites. A closer inspection makes visible a distinct gradation of Lewis acidity.

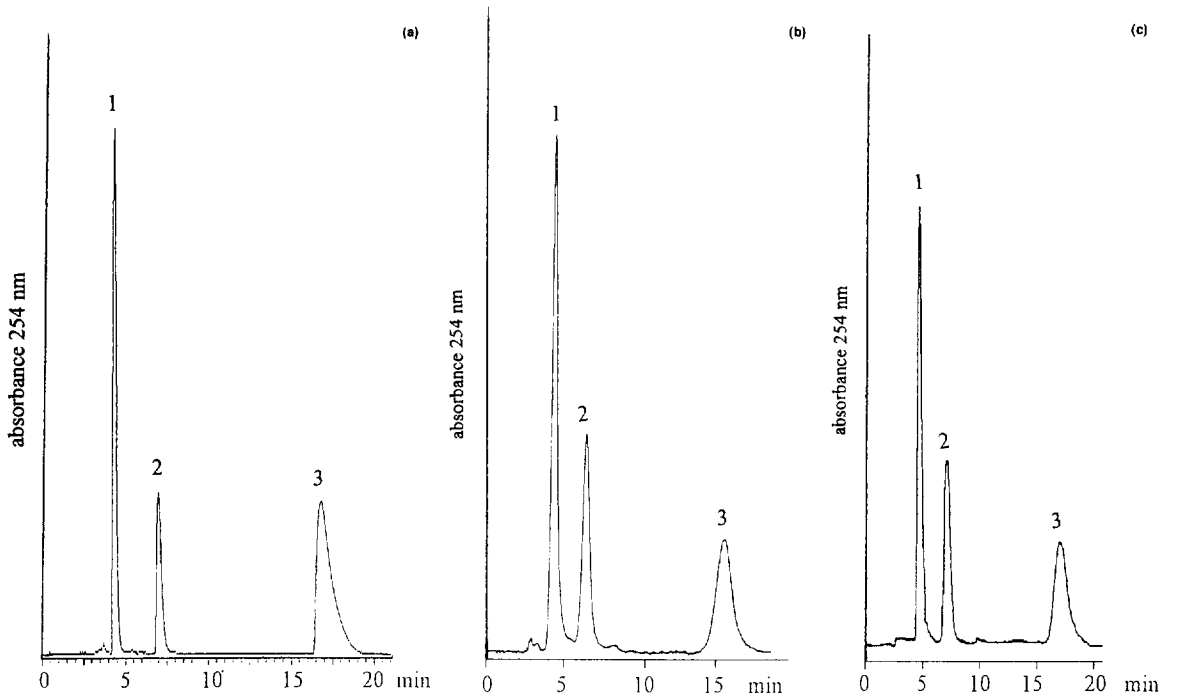

Fig. 2. Separation of anilines on LiChrospher Si 100 (a), MCM-41 (Si/Al=9) (b) and MCM-41 (Si/Al>1000) (c). Eluent: *n*-heptane–2-propanol (99.5:0.5, v/v). Flow-rate: 1 cm^3/min. UV detection at 254 nm. Injection volume: 20 mm^3. Peaks: 1=N,N-dimethylaniline; 2=N-methylaniline; 3=aniline.

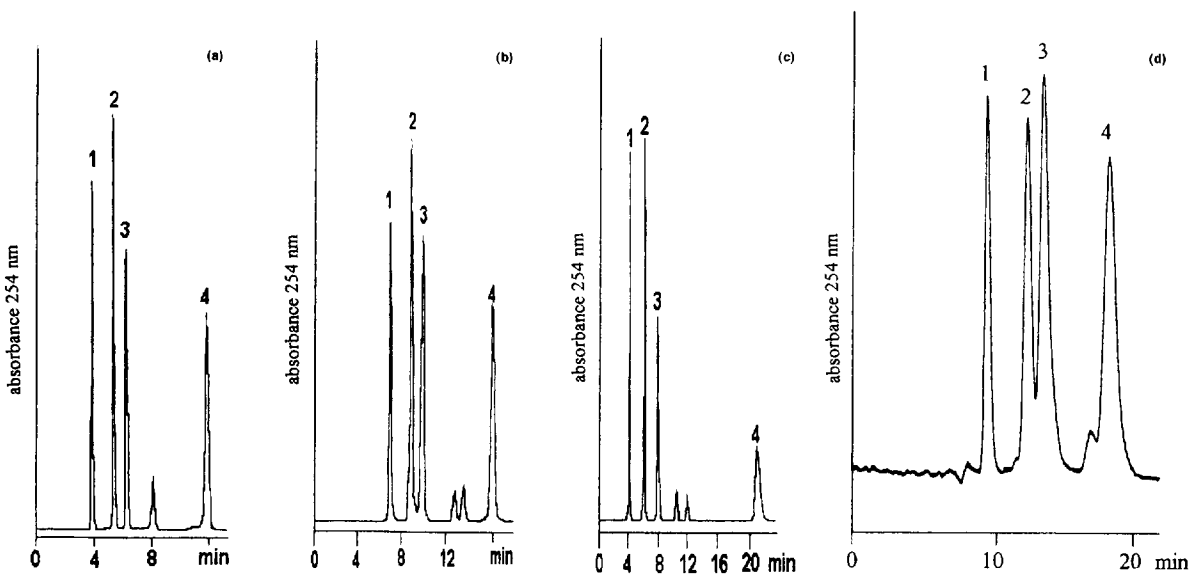

Fig. 3. Separation of polycyclic hydrocarbons on MCM-41 (Si/Al ratio=9) (a), alumina (b), titania (c), and zirconia (d). Columns: 250×4 mm. Eluent: π-pentane. Flow-rate: 1 cm^3/min. UV detection at 254 nm. Injection volume: 20 mm^3. Peaks: 1=naphtalene; 2=anthracene; 3=pyrene; 4=chrysene (a). 1=naphtalene; 2=anthracene; 3=chrysene; 4=benz[*a*]anthracene (b, c, d).

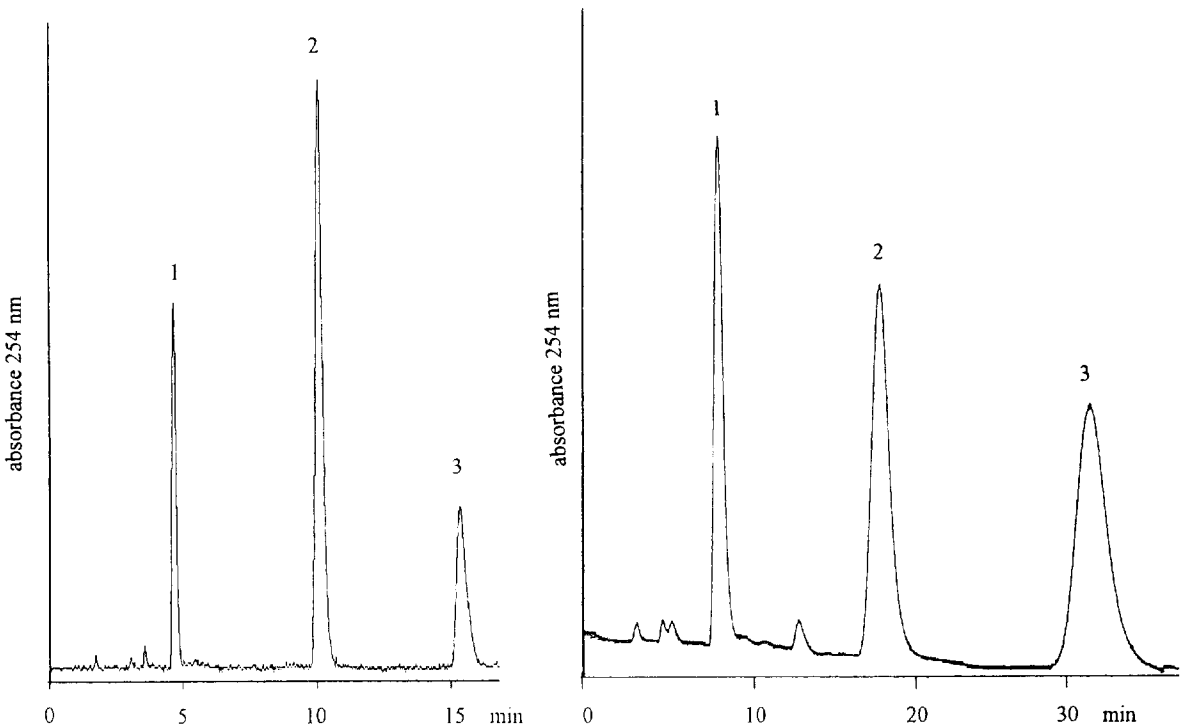

Fig. 4. Separation of phenols on LiChrospher Si 100 (a) and MCM-41 (Si/Al ratio=9) (b). Columns: 125×4 mm (a), 250×4 mm (b). Eluent: *n*-heptane–2-propanol (99.5:0.5, v/v). Flow-rate: 1 cm^3/min. UV detection at 254 nm. Injection volume: 20 mm^3. Peaks: 1=2,6-dimethylphenol; 2=2-methylphenol; 3=phenol.

Alumina exhibits the shortest retention times despite having the highest surface area, while zirconia shows the longest retention times indicating that zirconia has Lewis sites of the strongest acidity among these three oxides.

3.2.3. Separation of acid compounds

Fig. 4 shows the separation of various phenols on LiChrospher Si 100 (a) and MCM-41 (Si/Al ratio= 9) (b). Both packing materials exhibit nearly identical capacity fators and symmetrically shaped peaks. This behaviour can be assigned to the Broensted acidity of the silanol groups. Again the peak shape is nearly independent of the aluminium content of MCM-41. Zirconia, titania and alumina exhibit a strongly basic character and show much longer retention times and severely tailed peaks.

4. Conclusions

The behaviour of alumina, zirconia and titania in normal-phase chromatography is dominated by their basic character when separating basic and acid compounds.

Basic compounds show short retention times and symmetrical peaks on alumina, zirconia and titania. In contrast to those oxides, silica exhibits acid properties due to its silanol groups resulting in poorly shaped peaks and long retention times. The retention times on MCM-41 are comparable to those on silica but the symmetrical peaks are similar to those of alumina, zirconia and titania.

When separating acid compounds, silica has a clear advantage due to its Broensted acidity, whereas alumina, zirconia and titania show long retention times and poorly shaped peaks. The behaviour of

MCM-41 is similar to that of silica in terms of retention times and peak shapes.

The behaviour of alumina, titania and zirconia towards polycyclic aromatic hydrocarbons is determined by their strong Lewis acidity. A stepwise increase of Lewis acidity from alumina to zirconia is reflected by the increasing retention times. Silica shows almost no interactions resulting in short retention times. The most interesting feature of MCM-41 is the ability to separate all types of analytes (basic, acid and neutral) within acceptable retention times and good peak shapes. The versatility in separating acid and basic compounds may originate from formation of siloxane bridges during calcination leading to Lewis acidity and basicity and in the case of the alumosilicate, the Lewis acidity of the aluminium atoms. Also, the formation of alumina oxide hydrate in the pore channels of MCM-41 may lead to formation of Lewis acidity. It must be pointed out that the peak shape is nearly independent of the aluminium content of MCM-41.

References

[1] K.G. Van Landuyt, L.M. Tuyenpont, A.P. De Leenheer and D. Stöckl, J. Chromatogr. Sci., 32 (1994) 294.
[2] K. Cabrera, G. Jung, K. Czerny and D. Lubda, GIT Chromatographie, 11 (1991) 61.
[3] J. Nawrocki, M.P. Rigney, A. McCormick and P.W. Caw, J. Chromatogr. A, 657 (1993) 229.
[4] D.A. Hanggi and N.R. Marks, LC·GC Int., 11 (1993) 128.
[5] C.T. Kresge, M.E. Leonowicz, W.J. Roth, J.C. Vartuli and J.S. Beck, Nature, 359 (1992) 710.
[6] J.S. Beck, J.C. Vartuli, W.J. Roth, M.E. Leonowicz, C.T. Kresge, K.D. Schmitt, C.T.-W. Chu, D.H. Olson, E.W. Shepard, S.B. McCullen, J.B. Higgins and J.L. Schlenker, J. Am. Chem. Soc., 114 (1992) 10834.
[7] C.Y. Chen, H.X. Li and M.E. Davis, Microporous Mater., 2 (1993) 27.
[8] P.J. Branton, P.G. Hall, K.S.W. King, H. Reichert, F. Schüth and K.K. Unger, J. Chem. Soc., Faraday Trans. 1, 90 (1994) 2965.
[9] U. Ciesla, M. Grün, T. Isajeva, A.A. Kurganov, A.V. Neimark, P. Ravokovitch, S. Schacht, F. Schüth, K. Unger et al. in T.J. Pinnavaia and M.F. Thorpe (Editors), Access in Nanoporous Materials, Plenum Press, New York, 1995.
[10] A. Kurganov, U. Trüdinger, T. Isajeva and K. Unger, Chromatographia, 42 (1996) 217.
[11] U. Bollmann, Habilitationsschrift, Universität Freiberg, 1993.
[12] K. Unger, Porous Silica, Elsevier, Amsterdam, 1979.
[13] F. Schüth, Habilitationsschrift, Universität Mainz, 1994.
[14] N.E. Tretyakov, V.E. Filimonov, Kinet. Katal., 13 (1972) 815.
[15] M.L. Hair and W. Hertl, J. Phys. Chem., 74 (1970) 91.
[16] D.E. Yates, S. Levine and T.W. Healy, J. Chem. Soc., Faraday Trans. 1, 70 (1974) 1807.
[17] F. Schüth, Ber. Bunsenges. Phys. Chem., 99 (1995) 1306.
[18] A. Corma, A. Martinez, V. Martinez-Soria and J.B. Monton, J. Catal., 153 (1995) 25.
[19] P.I. Ravikovitch, S.C.Ó. Domhnaill, A.V. Neimark, F. Schüth and K.K. Unger, Langmuir, 11 (1995) 4765.